Modelling parametric down-conversion yielding spectrally pure photon pairs

Fabian Laudenbach,[1,2,*] **Hannes Hübel,**[1] **Michael Hentschel,**[1] **Philip Walther,**[2] **and Andreas Poppe**[1]

[1] *Optical Quantum Technology, Digital Safety and Security Department, AIT Austrian Institute of Technology GmbH, Donau-City-Straße 1, 1220 Vienna, Austria*

[2] *Quantum Optics, Quantum Nanophysics & Quantum Information, Faculty of Physics, University of Vienna, Boltzmanngasse 5, 1090 Vienna, Austria*

[*] *fabian.laudenbach.fl@ait.ac.at*

Abstract: Pair creation by spontaneous parametric down-conversion (SPDC) has become a reliable source for single-photon states, used in many kinds of quantum information experiments and applications. In order to be spectrally pure, the two photons within a generated pair should be as frequency-uncorrelated as possible. For this purpose most experiments use narrow bandpass filters, having to put up with a drastic decrease in count rates. This article elaborates (theoretically and by numerical evaluation) the alternative method to engineer a setup such that the SPDC-generated quantum states are intrinsically pure. Using pulsed pump lasers and periodically poled crystals this approach makes bandpass filtering obsolete and allows for significantly higher output intensities and therefore count rates in the detectors. After numerically scanning all common wavelength regimes, polarisation configurations and three different non-linear crystals, we present a broad variety of setups which allow for an implementation of this method.

OCIS codes: (270.0270) Quantum optics; (190.0190) Nonlinear optics; (270.5585) Quantum information and processing; (270.5565) Quantum communications; (190.4975) Parametric processes.

References and links

1. C. K. Hong, Z. Y. Ou, and L. Mandel, "Measurement of subpicosecond time intervals between two photons by interference," Phys. Rev. Lett. **59**, 2044 (1987).
2. P. J. Mosley, J. S. Lundeen, B. J. Smith, and I. A. Walmsley, "Conditional preparation of single photons using parametric downconversion: a recipe for purity," New J. Phys. **10**, 093011 (2008).
3. A. B. U'Ren, C. Silberhorn, R. Erdmann, K. Banaszek, W. P. Grice, I. A. Walmsley, and M. G. Raymer, "Generation of pure-state single-photon wavepackets by conditional preparation based on spontaneous parametric downconversion," http://arxiv.org/abs/quant-ph/0611019.
4. J. H. Eberly, "Schmidt analysis of pure-state entanglement," Laser Phys. **16**, 921–926 (2006).
5. R. B. Jin, R. Shimizu, K. Wakui, H. Benichi, and M Sasaki, "Widely tunable single photon source with high purity at telecom wavelength," Opt. Express **21**, 10659–10666 (2013).
6. P. G. Evans, J. Schaake, R. S. Bennink, W. P. Grice, and T. S. Humble, "Bright source of spectrally uncorrelated polarization-entangled photons with nearly single-mode emission," http://arxiv.org/abs/1009.1609.
7. A. Eckstein, A. Christ, P. J. Mosley, and C. Silberhorn, "Highly efficient single-pass source of pulsed single-mode twin beams of light," Phys. Rev. Lett. **106**, 013603 (2011).
8. K. Edamatsu, R. Shimizu, W. Ueno, R. B. Jin, F. Kaneda, M. Yabuno, H. Suzuki, S. Nagano, A. Syouji, and K. Suizu, "Photon pair sources with controlled frequency correlation," Prog. Inform. **8**, 19–26 (2011).
9. M. Yabuno, R. Shimizu, Y. Mitsumori, H. Kosaka, and K. Edamatsu, "Four-photon quantum interferometry at a telecom wavelength," Phys. Rev. A **86**, 010302 (2012).

#253363 Received 5 Nov 2015; revised 18 Dec 2015; accepted 5 Jan 2016; published 2 Feb 2016

10. R. B. Jin, K. Wakui, R. Shimizu, H. Benichi, S. Miki, T. Yamashita, H. Terai, Z. Wang, M. Fujiwara, and M. Sasaki, "Nonclassical interference between independent intrinsically pure single photons at telecommunication wavelength," Phys. Rev. A **87**, 063801 (2013).
11. R. B. Jin, R. Shimizu, I. Morohashi, K. Wakui, M. Takeoka, S. Izumi, T. Sakamoto, M. Fujiwara, T. Yamashita, S. Miki, H. Terai, Z. Whang, and M. Sasaki, "Efficient generation of twin photons at telecom wavelengths with 2.5 GHz repetition-rate-tunable comb laser," Sci. Rep. **4**, 7468 (2014).
12. S. Wollmann, M. Weston, H. M. Chrzanowski, S. Slussarenko, and G. Pryde, "High heralding efficiency single photon source at telecom wavelength," in *Proceedings of European Quantum Electronics Conference* (European Physical Society, 2015), EB-3.2-wed.
13. A. Smith, "SNLO," http://www.as-photonics.com/snlo.
14. M. V. Pack, D. J. Armstrong, and A. V. Smith, "Measurement of the $\chi(2)$ tensors of KTiOPO4, KTiOAsO4, RbTiOPO4, and RbTiOAsO4 crystals," Appl. Opt. **43**, 3319–3323 (2004).

1. Introduction

Spontaneous parametric down-conversion is a quantum-mechanical process where a photon of high energy (usually referred to as *pump*) spontaneously decays into two daughter photons (*signal* and *idler*) by interaction with a non-linear optical medium. In order for the three fields not to interfere destructively within the crystal, they can be phase-matched via the quasi-phase-matching technique, where the crystal is composed of thin layers with alternating non-linearity coefficient. This approach allows for phase-matching at any collinear three-wave mixing process. In general the frequency spectra of signal and idler are mutually correlated which negatively affects quantum purity. As pointed out in this article, this results in poor Hong-Ou-Mandel visibility [1] when two independent SPDC sources (or photons from different pairs of the same source) are used. By insertion of narrow bandpass filters into signal and idler channel the spectral correlations can be removed under the cost of discarding a better part of the down-converted photons and undermining heralding efficiency, as illustrated in Fig. 1(a). The approach discussed in this article aims to design the SPDC setup such that the output radiation is *a priori* uncorrelated, as depicted in Fig. 1(b), so no photons have to be discarded by filtering. This can be achieved by mutual matching of pulsed pump lasers (centre wavelength and spectral width) and periodically poled non-linear crystals (material, crystal type, poling periodicity, temperature). While the postulates of quantum mechanics, combined with numerical mathematics, show how the purity of down-converted photons can be evaluated [2–5], first experimental tests of this approach yielded promising results [5–12]. In our research we investigated phase-matching conditions and quantum state purity of all types of down-conversion in all common wavelength regimes and in three kinds of periodically poled crystals: *potassium titanyl phosphate* ($KTiOPO_4$, ppKTP), *lithium niobate* ($LiNbO_3$, ppLN) and *lithium tantalate* ($LiTaO_3$, ppLT).

#253363 Received 5 Nov 2015; revised 18 Dec 2015; accepted 5 Jan 2016; published 2 Feb 2016

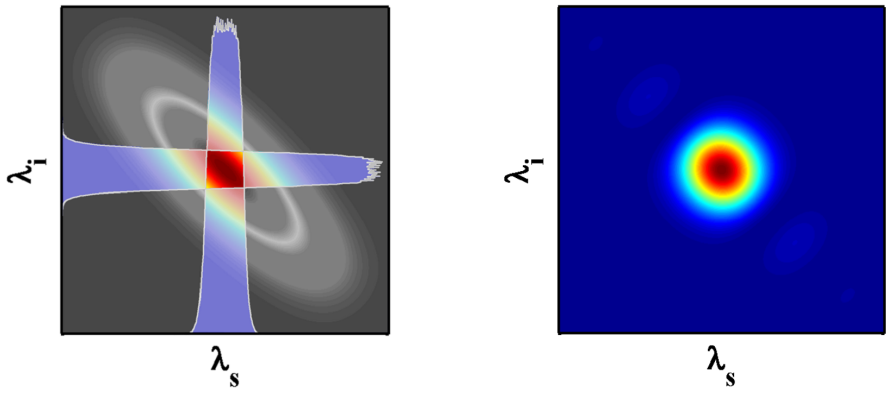

(a) (b)

Fig. 1. Sketch of the basic approach. Most experiments use narrow bandpass filters (a) to remove correlations in the joint spectral intensity, therefore omitting a significant amount of generated photons (grey area). Alternatively one can design the experimental setup such that the daughter spectra are intrinsically uncorrelated (b), hence no filters have to be used and no photons are discarded.

2. The SPDC amplitude

The quantum state that describes SPDC reads as

$$|\Psi\rangle = \tilde{\mathcal{N}} d_{\text{eff}} L \int_0^\infty \int_0^\infty \mu(\omega_s + \omega_i)\psi(\omega_s, \omega_i) a_s^\dagger a_i^\dagger \, d\omega_s \, d\omega_i \, |0\rangle \,, \tag{1}$$

where $\tilde{\mathcal{N}}$ is a normalisation constant, d_{eff} is the effective non-linearity coefficient of the crystal, L is the interaction length (i.e. the length of the non-linear crystal), $a_{s/i}^\dagger$ are the creation operators of a signal and idler photon respectively, μ is the pump envelope amplitude and ψ is the phase-matching envelope amplitude:

$$\psi(\omega_s, \omega_i) = e^{i\Delta\mathbf{k}L/2} \,\text{sinc}\left(\frac{\Delta\mathbf{k}L}{2}\right) \tag{2}$$

with $\Delta\mathbf{k}$ representing the phase-mismatch:

$$\Delta\mathbf{k} = 2\pi\left(\frac{n_p}{\lambda_p}\hat{\mathbf{k}}_p - \frac{n_s}{\lambda_s}\hat{\mathbf{k}}_s - \frac{n_i}{\lambda_i}\hat{\mathbf{k}}_i\right), \tag{3}$$

where $\lambda_{p/s/i}$ and $n_{p/s/i}$ are the wavelengths and refractive indices respectively. In the case of collinear quasi-phase-matching the mismatch reads

$$\Delta k = 2\pi\left(\frac{n_p}{\lambda_p} - \frac{n_s}{\lambda_s} - \frac{n_i}{\lambda_i} - \frac{m}{\Lambda}\right), \tag{4}$$

where m is an integer and Λ is the poling periodicity of the crystal. In order to achieve quasi-phase-matching, i.e. to reset the phase mismatch within the crystal periodically, the sign of the effective non-linearity d_{eff} is alternated in multiples of the length Λ. The refractive indices are subject to the wavelength- and temperature-dependent Sellmeier equations for respective crystal and polarisation direction. Therefore the phase-matching amplitude ψ is unique for each setup of down-conversion type, wavelengths, crystal and temperature.

#253363 Received 5 Nov 2015; revised 18 Dec 2015; accepted 5 Jan 2016; published 2 Feb 2016

3. Factorability

The Hong-Ou-Mandel visibility of two interfering substates ρ_A and ρ_B with respective purities P_A and P_B reads as [2]

$$V = \frac{P_A + P_B - \|\rho_A - \rho_B\|^2}{2}. \tag{5}$$

This equation illustrates nicely the role of state *purity P* and *indistinguishability* $\|\rho_A - \rho_B\|$ required for high visibilities. In our case *A* and *B* represent photons from two *independent* SPDC sources. (Note that Hong-Ou-Mandel interference of signal and idler from the *same* generated pair does not require high purity and is therefore not embraced in this paper.) Consider the special case of an interference experiment with two independent *identical* sources (or subsequent photons from the same source which is equivalent). If we let the two signal photons interfere and use the idler photons for heralding, the purities and the state operators of the interfering photons coincide ($P_A = P_B =: P$, $\rho_A = \rho_B$) and the visibility depends on the purity only:

$$V = P. \tag{6}$$

In the case where one pair's signal and the other pair's idler of are brought to interfere, the distinctness term $\|\rho_A - \rho_B\|$ does not necessarily cancel and the expression reads

$$V = P - \frac{\|\rho_s - \rho_i\|^2}{2}, \tag{7}$$

where we used the fact that for identical sources signal and idler carry the same purity, $P_s = P_i = P$, as derived below.

So no matter whether the experiment relies on interference of two signal photons or mutual interference of signal and idler, a high spectral purity P plays a key role in achieving high HOM-visibilities.

3.1. Pure and mixed states

The density operator of any quantum state reads

$$\rho = \sum_j p_j \left|\Psi_j\right\rangle \left\langle\Psi_j\right| \tag{8}$$

with $\sum_j p_j = 1$ and $|\Psi_j\rangle$ are pure quantum states. The operator ρ represents a pure state when there is only one non-vanishing p_j such that $\rho = |\Psi\rangle\langle\Psi|$, otherwise we speak of a mixed state. The purity of a state ρ is evaluated by tracing over its square:

$$P = \mathrm{Tr}(\rho^2) = \sum_j p_j^2. \tag{9}$$

In case of a bipartite quantum state ρ_{AB} we can trace over one subsystem in order to obtain the quantum state of the respective other subsystem:

$$\rho_A = \mathrm{Tr}_B\, \rho_{AB}, \qquad \rho_B = \mathrm{Tr}_A\, \rho_{AB}. \tag{10}$$

Any pure bipartite quantum state $|\Psi\rangle_{AB}$ can be expressed in terms of a shared complete set of orthonormal basis states:

$$|\Psi\rangle_{AB} = \sum_j \sqrt{\lambda_j}\, |\alpha_j\rangle_A \otimes |\beta_j\rangle_B. \tag{11}$$

#253363 Received 5 Nov 2015; revised 18 Dec 2015; accepted 5 Jan 2016; published 2 Feb 2016

This expression is known as the *Schmidt decomposition* of the state $|\Psi\rangle_{AB}$. The vectors $|\alpha_j\rangle_A$ and $|\beta_j\rangle_B$ are the so-called *Schmidt modes* of the respective subsystems and λ_j are the *Schmidt coefficients* which add up to one: $\sum_j \lambda_j = 1$. The pairs $|\alpha_j\rangle_A \otimes |\beta_j\rangle_B$ form a complete set of basis states of the total system. The Schmidt decomposition provides an intuitive measurement of entanglement within a pure state: If the state is entangled, then there is more than just one term present in Eq. (11).

When we build the density operator $\rho = |\Psi\rangle\langle\Psi|$ of the state (11) and perform a partial trace over the subsystem B we arrive after straightforward calculation at

$$\begin{aligned}
\mathrm{Tr}_B\,\rho_{AB} &= \sum_l \langle\beta_l|\,\rho_{AB}\,|\beta_l\rangle \\
&= \sum_l \langle\beta_l|\left(\sum_j\sum_k \sqrt{\lambda_j\lambda_k}\,|\alpha_j\rangle\langle\alpha_k|\otimes|\beta_j\rangle\langle\beta_k|\right)|\beta_l\rangle \\
&= \sum_l\sum_j\sum_k \sqrt{\lambda_j\lambda_k}\,|\alpha_j\rangle\langle\alpha_k|\otimes\langle\beta_l|\beta_j\rangle\langle\beta_k|\beta_l\rangle \\
&= \sum_l\sum_j\sum_k \sqrt{\lambda_j\lambda_k}\,|\alpha_j\rangle\langle\alpha_k|\otimes\delta^{lj}\delta^{kl} \\
&= \sum_j \lambda_j\,|\alpha_j\rangle\langle\alpha_j| = \rho_A. \qquad (12)
\end{aligned}$$

Comparing the above expression with Eq. (8) and (9) we find that the purity of the two subsystems is determined by their mutual Schmidt coefficients:

$$P_A = P_B = \mathrm{Tr}(\rho_A^2) = \mathrm{Tr}(\rho_B^2) = \sum_j \lambda_j^2. \qquad (13)$$

As we can see, the purity of the single photon states is, little surprising, proportional to the inverse degree of entanglement of the total state. In the case of a separable bipartite state

$$|\Psi\rangle = |\alpha\rangle\otimes|\beta\rangle \qquad (14)$$

there is only one non-vanishing Schmidt coefficient $\lambda = 1$ yielding maximum purity in both subsystems: $P_A = P_B = 1$.

3.2. Factorability of the SPDC amplitude

When we summarise pump and phase-matching envelope amplitude into a single function, the *joint spectral amplitude* (JSA)

$$f(\omega_s,\omega_i) = \mu(\omega_s+\omega_i)\,\psi(\omega_s,\omega_i), \qquad (15)$$

we can rewrite the amplitude for SPDC as

$$|\Psi\rangle = \mathscr{N}\int_0^\infty\int_0^\infty f(\omega_s,\omega_i)a_s^\dagger a_i^\dagger\,d\omega_s\,d\omega_i\,|0\rangle\,. \qquad (16)$$

The signal and idler quantum states are pure if the SPDC amplitude is separable, i.e. if it can be represented as

$$|\Psi\rangle = \mathscr{N}\int_0^\infty f_s(\omega_s)a_s^\dagger\,d\omega_s\int_0^\infty f_i(\omega_i)a_i^\dagger\,d\omega_i\,|0\rangle\,. \qquad (17)$$

However, the correlations of ω_s and ω_i in the joint spectral amplitude $f(\omega_s,\omega_i)$ *do* indicate a frequency entanglement of signal and idler photons. In order to investigate the entanglement

#253363 Received 5 Nov 2015; revised 18 Dec 2015; accepted 5 Jan 2016; published 2 Feb 2016

of the SPDC-amplitude $|\Psi\rangle$—a pure bipartite state—we would like to express it in terms of a Schmidt decomposition:

$$|\Psi\rangle = \sum_j \sqrt{\lambda_j}\, |s_j\rangle \otimes |i_j\rangle\,, \tag{18}$$

with Schmidt modes $|s_j\rangle$ and $|i_j\rangle$, representing the respective subsystems, signal and idler. We perform the Schmidt decomposition numerically by making a *singular value decomposition* (SVD) of the discretised JSA. For this purpose we first split the relevant range of signal and idler frequencies into discrete values $\omega_{s,m}$ and $\omega_{i,n}$. Then we express the state as a sum over all possible combinations of signal and idler eigenfunctions, $|\tilde{s}_m\rangle$ and $|\tilde{i}_n\rangle$, weighted by their respective joint amplitude $f(\omega_{s,m}, \omega_{i,n})$ each of which is calculated numerically:

$$|\Psi\rangle = \sum_m \sum_n f(\omega_{s,m}, \omega_{i,n})\, |\tilde{s}_m\rangle \otimes |\tilde{i}_n\rangle\,. \tag{19}$$

The amplitudes $f(\omega_{s,m}, \omega_{i,n})$ can be understood as components of an $M \times N$-matrix $\mathscr{F}$, each row (column) of which represents a particular discretised signal (idler) frequency:

$$f(\omega_{s,m}, \omega_{i,n}) = \langle \tilde{s}_m | \mathscr{F} | \tilde{i}_n \rangle = \langle \tilde{i}_n | \mathscr{F}^\dagger | \tilde{s}_m \rangle\,. \tag{20}$$

$\mathscr{F}\mathscr{F}^\dagger$ is the partial trace of the total state over the idler subsystem [4] which is in turn just the definition of the reduced density operator of the signal subsystem:

$$\mathscr{F}\mathscr{F}^\dagger = \sum_n \langle i_n | \rho | i_n \rangle = \rho_s. \tag{21a}$$

Analogously $\mathscr{F}^\dagger\mathscr{F}$ represents just the opposite:

$$\mathscr{F}^\dagger\mathscr{F} = \sum_m \langle s_m | \rho | s_m \rangle = \rho_i. \tag{21b}$$

We now express the respective amplitudes $f(\omega_{s,m}, \omega_{i,n})$ in Eq. (19) as components of $\mathscr{F}$ and obtain

$$|\Psi\rangle = \sum_m \sum_n \mathscr{F}^{mn}\, |\tilde{s}_m\rangle \otimes |\tilde{i}_n\rangle\,. \tag{22}$$

The SVD allows us to decompose any matrix into two unitary matrices U and $V^\dagger$ and a diagonal matrix D, such that

$$\mathscr{F} = UDV^\dagger, \tag{23}$$

where the columns of U represent the eigenvectors of $\mathscr{F}\mathscr{F}^\dagger = \rho_s$ and the columns of V (or rows of $V^\dagger$) are the eigenvectors of $\mathscr{F}^\dagger\mathscr{F} = \rho_i$. The entries in D are real, positive, appear in descending order on the diagonal and represent the eigenvalues of the eigenvectors described by the columns of U and V:

$$\mathscr{F}\mathscr{F}^\dagger U^{mj} = d_j U^{mj}, \tag{24a}$$

$$\mathscr{F}^\dagger\mathscr{F} V^{nj} = d_j V^{nj} = d_j \left(V^\dagger\right)^{jn}, \tag{24b}$$

#253363 Received 5 Nov 2015; revised 18 Dec 2015; accepted 5 Jan 2016; published 2 Feb 2016

where $d_j = D^{jj}$ are just the coefficients of the diagonal matrix. It is important to note that the j^{th} column of U and the j^{th} row of $V^\dagger$ are associated with the same eigenvalue d_j, i.e. the columns of U and V have a shared spectrum. We now replace $\mathscr{F}$ by its SVD representation, so Eq. (22) becomes

$$\begin{aligned}
|\Psi\rangle &= \sum_m \sum_n \left(UDV^\dagger\right)^{mn} |\tilde{s}_m\rangle \otimes |\tilde{i}_n\rangle \\
&= \sum_j \sum_m \sum_n U^{mj} D^{jj} \left(V^\dagger\right)^{jn} |\tilde{s}_m\rangle \otimes |\tilde{i}_n\rangle \\
&= \sum_j d_j \left(\sum_m U^{mj} |\tilde{s}_m\rangle\right) \otimes \left(\sum_n \left(V^\dagger\right)^{jn} |\tilde{i}_n\rangle\right). \qquad (25)
\end{aligned}$$

So we expressed the state $|\Psi\rangle$ in terms of a complete set of basis states, each weighted by a coefficient d_j. As long as the squares of the coefficients sum up to one, this is just the unique expression for the Schmidt decomposition of $|\Psi\rangle$. So after D has been normalised such that $\sqrt{\text{Tr}(D^2)} = 1$ we can identify its entries with the Schmidt coefficients: $d_j = \sqrt{\lambda_j}$. Furthermore we define

$$|s_j\rangle = \sum_m U^{mj} |\tilde{s}_m\rangle\,, \qquad (26a)$$

$$|i_j\rangle = \sum_n \left(V^\dagger\right)^{jn} |\tilde{i}_n\rangle\,, \qquad (26b)$$

yielding the desired expression (18). The purity of ρ_s and ρ_i can then be easily obtained by Eq. (9), only using the entries d_j of the diagonal matrix D.

Experimentally, a separable JSA can be achieved by appropriate matching of the pulse duration and the crystal length. Fig. 2(a) depicts the *joint spectral intensity* $|f(\omega_s, \omega_i)|^2$ (JSI) in the case of a narrow-band CW laser impinging a short crystal, resulting in anti-correlated signal and idler spectra. Conversely, a broadband femtosecond laser impinging a long crystal would result in correlated daughter photons as shown in Fig. 2(b). When pulse duration and crystal length are mutually matched, we can achieve frequency-uncorrelated signal and idler spectra as illustrated in Fig. 2(c) and Fig. 2(d).

#253363 Received 5 Nov 2015; revised 18 Dec 2015; accepted 5 Jan 2016; published 2 Feb 2016

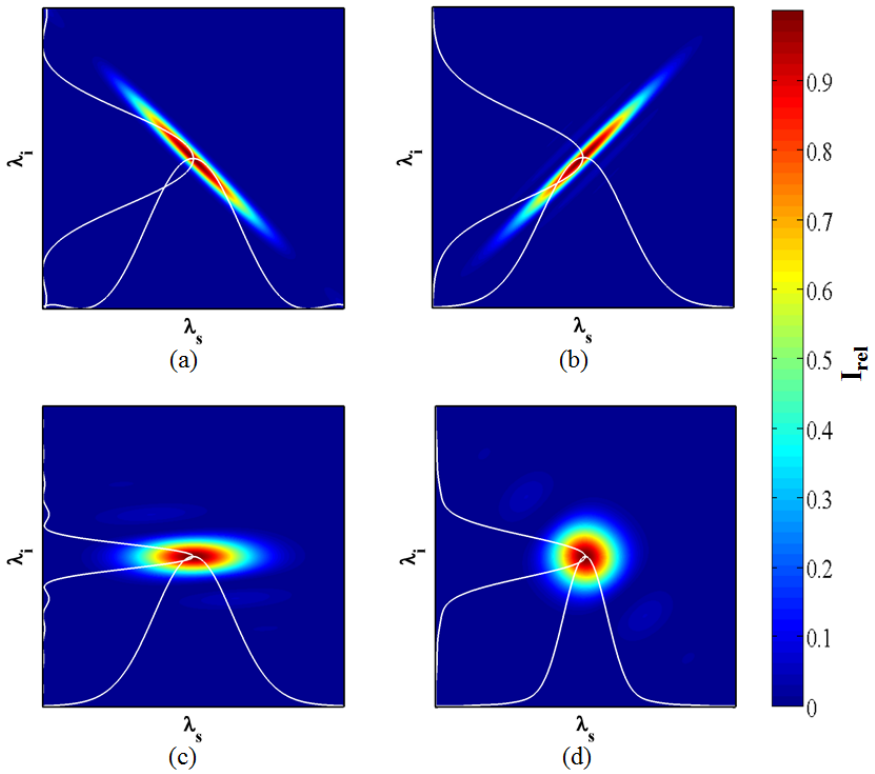

Fig. 2. Graphical representation of the joint spectral intensity in four different configurations. In the case of coinciding centre wavelengths ($\lambda_s = \lambda_i$) Figs. (a), (b) and (d) each represent spectrally indistinguishable signal and idler radiation. However, Figs. (a) and (b) depict cases where signal and idler wavelengths are highly (anti-) correlated, resulting in a purity of $P \sim 0.1$. The plots on the bottom each illustrate a frequency-uncorrelated down-conversion ($P \sim 1$), where signal and idler carry (c) different and (d) same bandwidth respectively (as indicated by the white curves).

4. Numerical evaluation

Unfortunately, the generation of intrinsically pure quantum states is only possible for a limited amount of setups; as pointed out above, the JSA depends on the mutual relation of pump envelope intensity and phase-matching envelope intensity. The latter depends ultimately on the material's Sellmeier equations which provide the refractive index for a given polarisation, wavelength and temperature. As it turns out, each crystal allows for generation of intrinsically pure down-converted photons only in the case of very specific polarisation- and wavelength configurations.

Using numerical calculations we investigated the suitability of three periodically poled nonlinear crystals, potassium titanyl phosphate (KTP), lithium niobate (LN) and lithium tantalate (LT), for all kinds of down-conversion processes which carry a non-vanishing effective non-linearity (Table 1). (All calculations were performed using our own Matlab-based program `QPMoptics` which is available from the authors.) This systematic and extensive search for setups which allow for generation of intrinsically pure quantum states is—to our knowledge—unprecedented so far. This way we were able not only to confirm the choice of specific crystals in recent experiments but also to find other promising (type 0, I and II) setups that

#253363 Received 5 Nov 2015; revised 18 Dec 2015; accepted 5 Jan 2016; published 2 Feb 2016

were previously unknown and will be presented in the succeeding subsections. (For the sake of a concise presentation we here omit the discussion of configurations with very low effective non-linearity, namely $o \longrightarrow o+o$, $e \longrightarrow o+o$ and $o \longrightarrow o+e$ in LT. Moreover, our calculations revealed that there are no opportunities for designing a setup with intrinsically pure daughter states exploiting type I SPDC in ppKTP. Therefore this setup will neither be discussed any further in this paper.)

Table 1. Effective non-linearity coefficients for all polarisation configurations and three kinds of periodically poled crystals. In all cases a collinear propagation along the crystal's x-axis is assumed. The letter o denotes polarisation along the *ordinary* (the y-) axis while e denotes polarisation along the *extraordinary* (the z-) axis. Note that all numerical values in the table are to be understood as approximation since they vary slightly with the involved wavelengths and the material's doping. The values are taken from the software *SNLO v63*, developed by *AS-Photonics, LLC* [13].

SPDC Type		Effective Non-Linear Coefficient $\lvert d_{\text{eff}}\rvert$ $\left[\text{pmV}^{-1}\right]$		
		ppKTP	ppLN	ppLT
0	$o \longrightarrow o+o$	0	$d^{22} \sim 1.5$	$d^{22} \sim 0.9$
	$e \longrightarrow e+e$	$d^{33} \sim 9.4$	$d^{33} \sim 14.5$	$d^{33} \sim 7.6$
I	$o \longrightarrow e+e$	0	0	0
	$e \longrightarrow o+o$	$d^{24} \sim 2.4$	$d^{31} \sim 2.8$	$d^{31} \sim 0.3$
II	$o \longrightarrow o+e$	$d^{32} \sim 2.4$	$d^{31} \sim 2.8$	$d^{31} \sim 0.3$
	$e \longrightarrow o+e$	0	0	0

4.1. Parallel polarisation

In order to generate photon pairs with same polarisation, down-conversions of type 0 and type I can be used. Type 0 SPDC with polarisations $e \longrightarrow e+e$ gives access to the effective non-linearity coefficient $d_{\text{eff}} = d^{33}$ which carries by far the highest value in all three crystals. Setups which allow for intrinsically pure type 0 SPDC are depicted in Fig. 3. As the plots show, these setups generate photons with signal or/and idler in the mid-infrared regime and are therefore of little relevance due to poor detection efficiencies. However, type I down-conversion ($e \longrightarrow o+o$) in ppLN, depicted in Fig. 4, does offer configurations of low spectral correlation with wavelengths which are more accessible for today's detectors.

The plots in Figs. 3 and 4 depict wavelength configurations which are promising regarding spectrally uncorrelated daughter states. Note however that, as an additional requirement for high purity, the laser's bandwidth and the crystal length have to be matched to each other. The dependence of purity on these parameters varies with the involved wavelengths and has to be evaluated for each individual setup. As an example, Fig. 5 illustrates the function $P(\tau, L)$ for the type I down-conversion $750\,\text{nm} \longrightarrow 1200\,\text{nm} + 2000\,\text{nm}$ in ppLN.

#253363 Received 5 Nov 2015; revised 18 Dec 2015; accepted 5 Jan 2016; published 2 Feb 2016

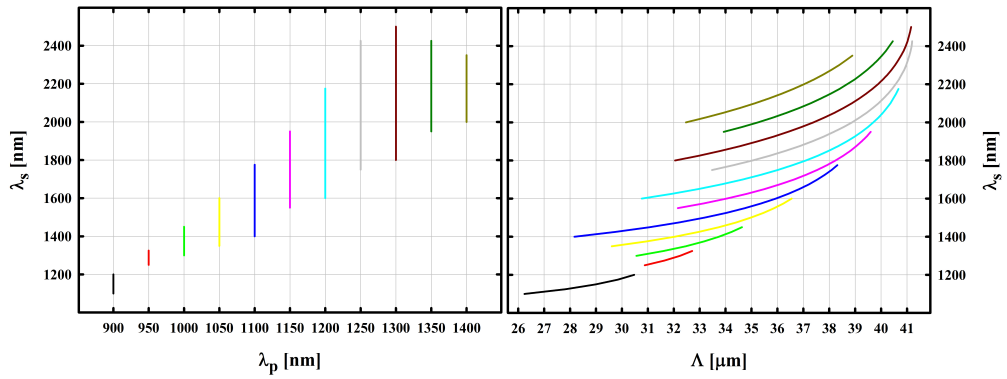

(a) ppKTP, $e \longrightarrow e+e$, $d_{\text{eff}} \sim 9.4\,\text{pmV}^{-1}$

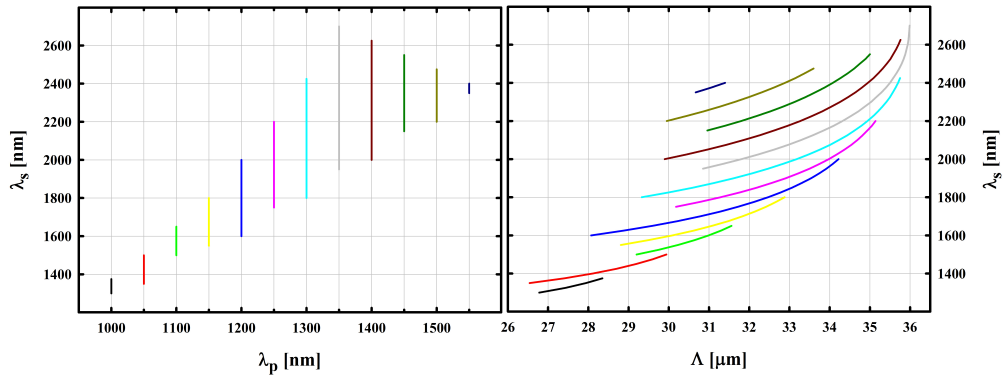

(b) ppLN, $e \longrightarrow e+e$, $d_{\text{eff}} \sim 14.5\,\text{pmV}^{-1}$

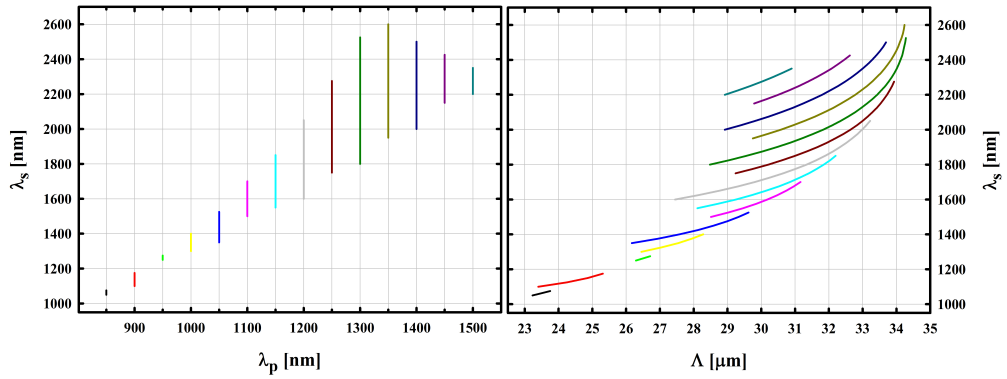

(c) ppLT, $e \longrightarrow e+e$, $d_{\text{eff}} \sim 7.6\,\text{pmV}^{-1}$

Fig. 3. Signal wavelength versus pump wavelength λ_p (left) and crystal periodicity Λ (right) for type 0 SPDC in (a) ppKTP, (b) ppLN and (c) ppLT. All plots exclusively display configurations which allow for an uncorrelated joint spectral intensity. Each coloured line corresponds to a certain pump wavelength λ_p and depicts the range of signal wavelength over which an intrinsic purity of more than 0.99 can be achieved by mutual matching of pump spectrum and crystal length. Note that all depicted data corresponds to a crystal temperature of 50 °C and is slightly modified with varying temperature.

#253363 Received 5 Nov 2015; revised 18 Dec 2015; accepted 5 Jan 2016; published 2 Feb 2016

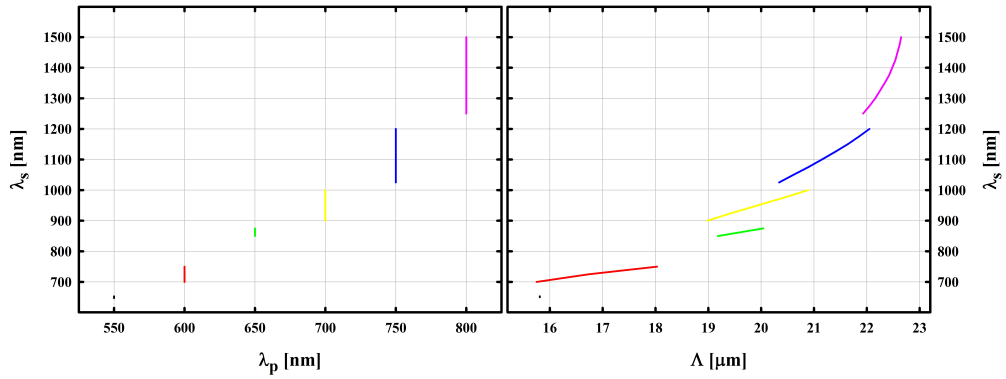

Fig. 4. Setups for intrinsically pure state generation in ppLN, SPDC type I $e \longrightarrow o + o$ and effective non-linearity $d_{\text{eff}} = d^{31} \sim 2.8\,\text{pmV}^{-1}$. The down-conversion 750 nm $\longrightarrow$ 1200 nm + 2000 nm is closer investigated in Fig. 5 as an exemplary illustration of how pulse duration and crystal length have to be mutually matched for high purity.

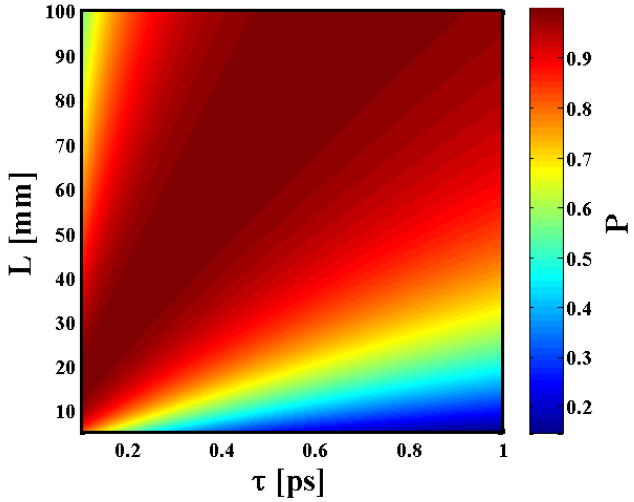

Fig. 5. Illustration of the spectral purity P with respect to pulse duration τ and crystal length L in the case of a type I down-conversion from 750 nm to 1200 nm and 2000 nm in ppLN.

#253363 Received 5 Nov 2015; revised 18 Dec 2015; accepted 5 Jan 2016; published 2 Feb 2016

4.2. *Orthogonal polarisation*

Figure 6 depicts configurations of type II SPDC in ppKTP and ppLN which allow for generation of spectrally uncorrelated daughter photons. It turns out however that for periodically poled lithium niobate the generated photons carry wavelengths which are—in the single photon regime—almost impossible to detect with satisfying efficiency. As seen in the right plot in Fig. 6(a) the required poling periodicity of KTP crystals approaches infinity for a specific set of wavelength configurations. This feature opens opportunities for phase matched *and* intrinsically uncorrelated spectra *without periodic poling* of the crystal. The advantages of this property range from cost savings to higher SPDC efficiencies since the effective non-linear coefficient $d_{\text{eff}} = d^{24}$ in bulk KTP goes up as high as to $3.9\,\text{pmV}^{-1}$ [14] compared to $2.3\,\text{pmV}^{-1}$ in ppKTP. A depiction of all possible pump- and signal wavelength configurations which do not require periodic poling can be found in Fig. 7. Unfortunately, as the plot indicates, the generated wavelengths lie in areas which are difficult to detect with common avalanche photodiodes ($\lambda_s = 1000$–$2200\,\text{nm}$, $\lambda_i = 1800$–$3200\,\text{nm}$). Future developments and upcoming detection technologies, i.e. superconducting nanowire detectors, might soon make them more accessible.

Photon pairs which carry the same centre wavelength but orthogonal polarisation find many applications in quantum-based experiments. We therefore subjected the crystals to an in-depth investigation to find out about their properties in frequency-degenerate type II down-conversion ($\lambda_s = \lambda_i = 2 \times \lambda_p$, $o \longrightarrow o + e$). As illustrated by the grey lines in Fig. 6, both crystals, ppKTP and ppLN, offer many opportunities for the case of frequency-degenerate pure quantum states. However, in order to achieve maximum spectral indistinguishability of signal and idler, the daughter fields should not only carry the same centre wavelength but also the same bandwidth. Fig. 8 shows a plot of configurations with phase-matched and pure output states in ppKTP for which $\lambda_s = \lambda_i = 2 \times \lambda_p$. The plot illustrates that signal and idler states are—although pure—in general spectrally distinguishable due to their different bandwidths (compare Fig. 2(c)) which undermines visibilities in interference experiments. However, in the telecom regime (located in the neighbourhood of $\lambda_p = 770$–$800\,\text{nm}$) the output spectra turn out to coincide sufficiently for most applications which justifies the choices that were made in recent experiments [5–12]. Maximal spectral indistinguishability can be achieved at the down-conversion $791\,\text{nm} \longrightarrow 2 \times 1582\,\text{nm}$. In the case of frequency-degenerate SPDC in ppLN we found the point of coinciding wavelengths *and* bandwidths to lie at $1755\,\text{nm} \longrightarrow 2 \times 3510\,\text{nm}$. These wavelengths can be regarded as material constants of the respective non-linear materials.

Given a configuration of wavelengths, polarisations and crystal that in principle allow for generation of intrinsically uncorrelated daughter fields, the pulse duration τ and crystal length L have to be mutually matched to achieve high purity in the laboratory. Fig. 9 depicts how the purity behaves with respect to τ and L in two different examples, $791\,\text{nm} \longrightarrow 2 \times 1582\,\text{nm}$ in ppKTP and $650\,\text{nm} \longrightarrow 1011\,\text{nm} + 1820.36\,\text{nm}$ in bulk KTP.

#253363 Received 5 Nov 2015; revised 18 Dec 2015; accepted 5 Jan 2016; published 2 Feb 2016

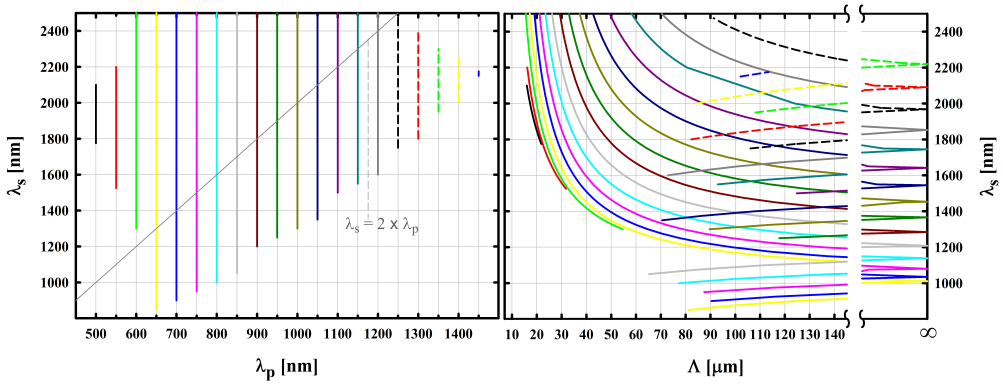

(a) ppKTP, $o \longrightarrow o+e$, $d_{\text{eff}} = d^{32} \sim 2.4\,\text{pmV}^{-1}$

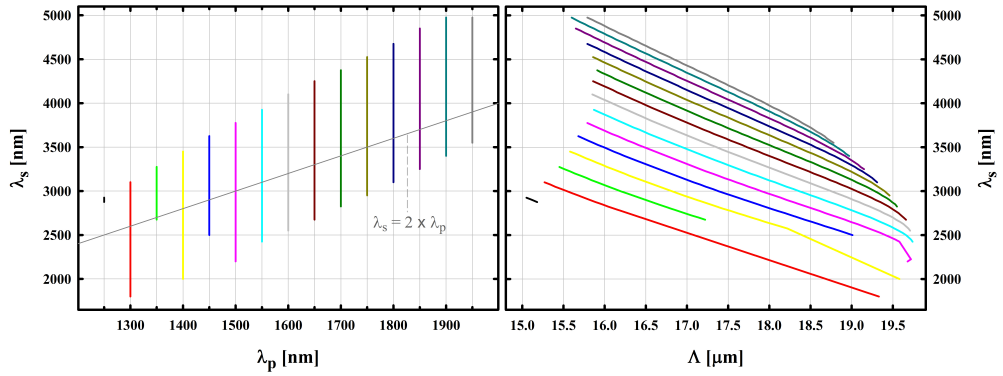

(b) ppLN, $o \longrightarrow o+e$, $d_{\text{eff}} = d^{31} \sim 2.8\,\text{pmV}^{-1}$

Fig. 6. Signal wavelength versus pump wavelength λ_p (left) and crystal periodicity Λ (right) for type II SPDC in (a) ppKTP and (b) ppLN at $T = 50\,^{\circ}\text{C}$. Again, only setups which allow for intrinsically pure signal and idler states are displayed. The gray line in the left plots represents spectrally symmetric down-conversions. For ppKTP there is a range of pump and signal wavelengths for which the periodicity approaches infinity (as indicated schematically by the convergent lines after the axis break). This property enables spectrally pure output generation without periodic poling (displayed in Fig. 7). Moreover, Fig. (a) illustrates that ppKTP allows for pure degenerate output states with signal and idler in the telecom band. Fig. (b) indicates that ppLN allows for *a priori* uncorrelated spectra only with signal and idler in the mid-infrared regime.

#253363 Received 5 Nov 2015; revised 18 Dec 2015; accepted 5 Jan 2016; published 2 Feb 2016

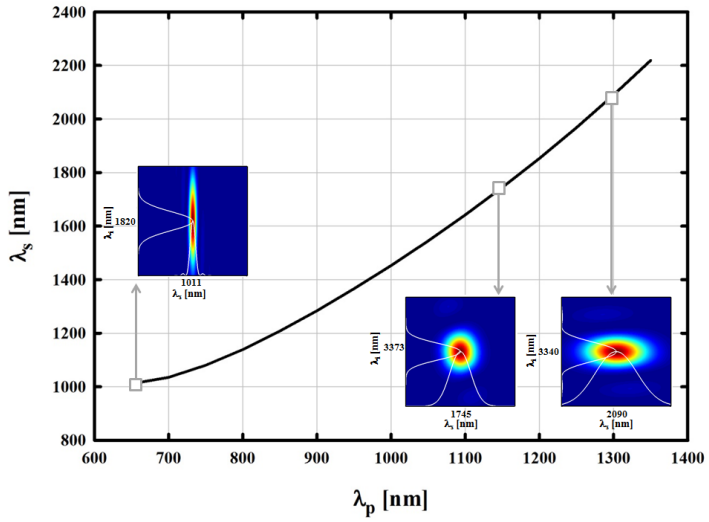

Fig. 7. Illustration of setups for type II SPDC ($o \longrightarrow o+e$) which allow for phase-matched and intrinsically pure states in bulk—not periodically poled—KTP ($d_{\text{eff}} \sim 3.9\,\text{pmV}^{-1}$ [14]). The JSI of three setups is depicted via insets as examples. The down-conversion 650 nm $\longrightarrow$ 1011 nm + 1820.36 nm is closer investigated in Fig. 9(b).

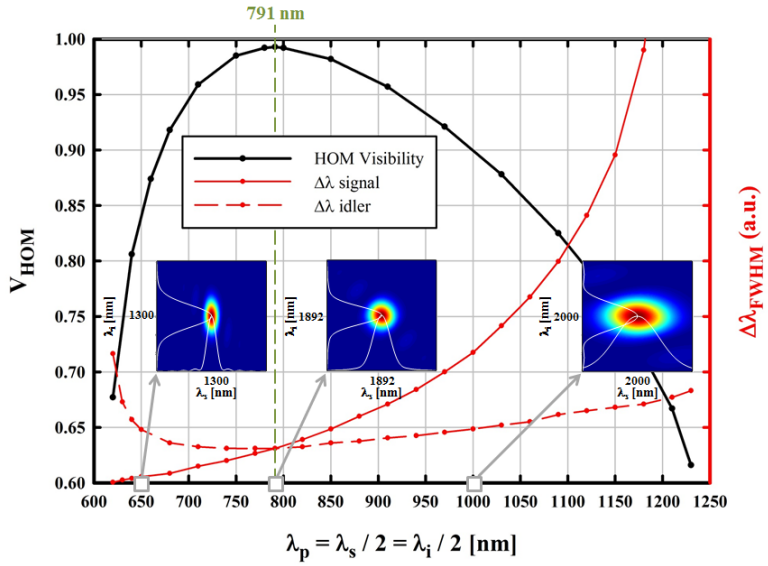

Fig. 8. Pure quantum-state generation by frequency-degenerate type II SPDC ppKTP. The black curve depicts the Hong-Ou-Mandel visibility between signal and idler of one source. The red curves illustrate how signal and idler bandwidths change relatively to each other with respect to λ_p (here in arbitrary units since the numeral values of $\Delta\lambda_{s/i}$ depend on the respective pulse- and crystal lengths). Although pure states can be generated within the full plotted range, signal and idler are fully spectrally indistinguishable only at the down-conversion 791 nm $\longrightarrow 2 \times 1582$ nm, as indicated by the intersection of the red curves.

#253363
Received 5 Nov 2015; revised 18 Dec 2015; accepted 5 Jan 2016; published 2 Feb 2016

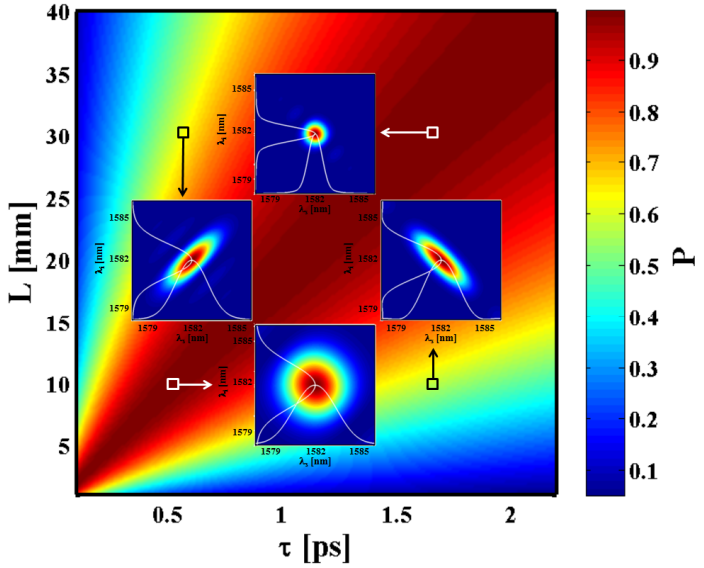

(a) ppKTP, 791 nm $\longrightarrow 2 \times 1582$ nm,
ppLN, 1755 nm $\longrightarrow 2 \times 3510$ nm

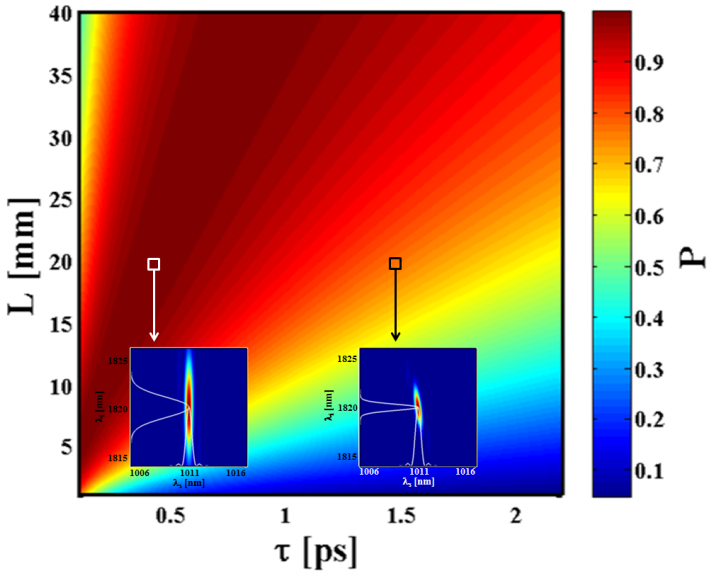

(b) KTP, 650 nm $\longrightarrow$ 1011 nm + 1820.36 nm

Fig. 9. Tailoring spectrally uncorrelated output states by mutual matching of pulse duration τ and crystal length L. The graphs illustrate three examples of type II SPDC: Fig. (a) represents frequency-degenerate SPDC with 791 nm pump in ppKTP (similar plot for 1755 nm pump in ppLN); Fig. (b) represents type II down-conversion 650 nm $\longrightarrow$ 1011 nm + 1820.36 nm in *bulk* KTP. Note from the insets how the output spectra get narrower with increasing crystal- and pulse length.

#253363 Received 5 Nov 2015; revised 18 Dec 2015; accepted 5 Jan 2016; published 2 Feb 2016

5. Conclusion

We discussed, analytically and numerically, the generation of photon pairs with high spectral purity, circumventing the need for bandpass filtering. We presented a broad variety of SPDC setups that allow for intrinsically pure quantum states most of which were unknown so far. We could confirm the well known property of ppKTP with $\Lambda \sim 46\,\mu\text{m}$ to generate uncorrelated daughter photons with SPDC in the vicinity of $780\,\text{nm} \longrightarrow 2 \times 1560\,\text{nm}$ with the maximal spectral indistinguishability being located at $791\,\text{nm} \longrightarrow 2 \times 1582\,\text{nm}$. For type II SPDC in ppLN we found the point of maximum spectral purity and indistinguishability to lie at $1755\,\text{nm} \longrightarrow 2 \times 3510\,\text{nm}$. Moreover, we presented a variety of novel configurations with high intrinsic purity. Among others we discussed how KTP allows for generation of phase-matched and pure daughter fields without periodic poling, which gives rise to significant advantages such as cost savings and higher count rates.

Acknowledgments

This work was funded by the Austrian Research Promotion Agency (Österreichische Forschungsförderungsgesellschaft, FFG; contract: 4642983, 'KVQ'). Furthermore, we thank the members of the Philip Walther group at the University of Vienna for technical support and fruitful discussions and advice. P.W. acknowledges support from the European Commission with the projects EQuaM (No. 323714), GRASP (No. 613024), PICQUE (No. 608062), QuILMI (No. 295293) and QUCHIP (No. 641039) as well as the Austrian Science Fund (FWF) with the projects PhoQuSi (Y585-N20) and the doctoral programme CoQuS Complex Quantum Systems (W1210-N16).

#253363 Received 5 Nov 2015; revised 18 Dec 2015; accepted 5 Jan 2016; published 2 Feb 2016